

Solubility of Refrigerant 1,1,1,2-Tetrafluoroethane in the *N,N*-Dimethyl Formamide in the Temperature Range from (263.15 to 363.15) K

Xiaohong Han, Zanjun Gao, Yingjie Xu, Yu Qiu, Xuwei Min, Xiaolong Cui, and Guangming Chen*

Institute of Refrigeration and Cryogenics, Zhejiang University, Hangzhou 310027, China

ABSTRACT: The solubility of the refrigerant in the solvent has an important effect on the efficiency of absorption refrigeration. In this paper, the solubility of 1,1,1,2-tetrafluoroethane (HFC-134a) in *N,N*-dimethyl formamide (DMF) was measured from $T = (263.15 \text{ to } 363.15) \text{ K}$. Throughout the observation of overall experiment, there was no stratification and no sediment generated, and the color of liquid had no change in the equilibrium cell before and after the experiment. The above-mentioned content suggested that any ratio of HFC-134a and DMF could be miscible. The experimental data were correlated by the activity coefficient model—NRTL model. The results show a good agreement with the experimental data. The overall average relative deviation of the pressure is 1.9 %, and the maximum relative deviation of the pressure is 5.2 %. Meanwhile, the results reveal that DMF shows very high affinity with HFC-134a because the mole fraction of HFC-134a in DMF at a specific temperature and pressure is higher (negative deviation) than that predicted for an ideal solution obeying Raoult's law.

INTRODUCTION

Absorption refrigeration systems have been used more and more in recent years because they can be driven by a low thermal potential energy source, such as solar energy or industrial waste steam. Besides the ammonia–water and water–lithium bromide refrigerant–absorbent pairs presently commercially utilized, numerous other refrigerant–absorbent pairs are currently being considered.^{1–5} Among these, fluorocarbon-based refrigerants, together with suitable nonvolatile organic solvents such as dimethylether of tetraethylene glycol (DMETEG), dibutyl phthalate (DBPh), and *N,N*-dimethylformamide (DMF) appear to be promising. Compared with DMETEG and DBPh, DMF has several advantages, such as considerably lower price, significantly lower viscosity, and strong absorption capacity (in the absorption refrigeration system, the absorptor should have a strong ability to absorb the refrigerant) for hydrochlorofluorocarbons (HCFCs).⁶

Literature reviews indicated that chlorodifluoromethane (HCFC-22) was the best fluorocarbon refrigerant for use in absorption refrigeration systems.^{6–8} HCFC-22 with organic solvents had been studied by some researchers.^{3–8} However, as a result of regulation of chlorofluorocarbons (CFCs) and hydrochlorofluorocarbons (HCFCs), hydrofluorocarbons (HFCs) and mixtures of these fluids are being investigated as alternative refrigerants.^{9–12}

The normal boiling points of 1,1,1,2-tetrafluoroethane (HFC-134a) and DMF are (247.08 and 426.20) K, respectively. Thus, the difference in boiling points is large (of the order of 180 K) which is desirable for absorption refrigeration systems, both for space conditioning and refrigeration applications. Also, both the components are chemically stable over the entire temperature range used in the absorption refrigeration systems. Thus, DMF (absorbent) and HFC-134a (refrigerant) seem to form one of the most promising combinations for the absorption refrigeration system. To characterize the performance of the working pair

HFC-134a + DMF, reliable $p-T-x$ data are needed over a wide temperature and composition range for the refrigeration system. Zehioua¹³ measured the isothermal vapor–liquid equilibrium (VLE) data of HFC-134a + DMF at (303.3, 318.18, 323.34, 338.26, and 354.24) K. In this work, the solubility data for the binary system HFC-134a + DMF from $T = (263.15 \text{ to } 363.15) \text{ K}$ at 10 K intervals and over a complete range of compositions were measured in an equilibrium apparatus to extend the measuring range of the literature.¹³ Experimental data were correlated by the NRTL model. The solubility data of HFC-134a were used to determine the activity coefficient of HFC-134a in the refrigerant–absorbent solutions. The effects of DMF on the solubility of HFC-134a and the properties of the solutions are discussed.

EXPERIMENTAL SECTION

Chemicals. HFC-134a was supplied by Honeywell Inc. (USA) with a mass purity of > 99.9 %. DMF was supplied by SamSung Fine Chemical Co. Ltd. (Korea) with a mass purity of > 99.99 %. Both samples were used without any further purification, and the critical parameters of DMF¹⁴ and HFC-134a¹⁵ are shown in Table 1.

Apparatus. The experimental apparatus used to measure the solubility of HFC-134a is shown in Figure 1. The apparatus includes a thermostat bath, an equilibrium cell, temperature and pressure controllers, and measurement devices. The equilibrium cell which was made of stainless steel with an inner volume of about 80 cm³ was immersed in the thermostat bath. In its middle part, a pair of Pyrex glass windows of 20 mm thickness was installed so that phase behaviors could be observed during the operation.

Received: August 2, 2010

Accepted: March 13, 2011

Published: April 21, 2011

The temperature of the equilibrium cell in the thermostat bath was maintained by the refrigeration subsystem and heater subsystem. The temperature measurement was made with a standard platinum resistance thermometer (25 Ω Yunnan Instrument) with an uncertainty of ± 10 mK (ITS) and a Keithley 2010 data acquisition/switch unit. The overall temperature uncertainty for the measurement system was less than ± 15 mK.

When the pressure of the system was below 120 kPa, it was directly measured by the absolute pressure transducer (Druck PTX-610), and the total uncertainty was within ± 0.05 kPa. When the system pressure was above 120 kPa, its pressure was measured by the pressure transducer (Druck PMP4010), combined with a differential pressure null transducer (Xi'an Instrument, 1151DP), an oil-piston type dead-weight pressure gauge (Xi'an Instrument, YS-60), and an atmospheric pressure gauge (Ningbo Instrument, DYM-1). The whole pressure measurement system had an uncertainty of ± 1.6 kPa.

In this paper, the mass of the mixture (refrigerant and DMF) was determined by weighting the DMF and refrigerant in electronic scales (model: BS4000S, from Beijing Sartorius

(Sartorius) Limited company, its full scale: 4010 g and its uncertainty: 0.01 g), respectively.

The mass fraction of refrigerant in the liquid phase

$$w_R = \frac{m_R - m_{V,R}}{m_R + m_{DMF} - m_{V,R}} \quad (1)$$

where m_{DMF} is the mass of DMF; m_R is the additive refrigerant mass; and $m_{V,R}$ is the vapor-phase refrigerant mass in the equilibrium cell.

The mass m_{DMF} and m_R were determined on an electronic scale, with an uncertainty of 0.01 g, and the mass of refrigerant in the vapor phase was obtained by the following equation

$$m_{V,R} = \rho V \quad (2)$$

where ρ is the refrigerant density in the vapor phase, obtained by REFPROP¹⁵, and the vapor phase refrigerant volume V consists of two parts, stainless steel pipe volume V_1 and the upper vapor space volume V_2 in the equilibrium cell. In this paper, vapor measurement uncertainty of total volume is ± 1.15 cm³, and the total uncertainty of x_R is ± 0.002 , where x_R is the liquid mole fraction of the refrigerant.

Experimental Procedures. The system was first evacuated to remove inert gases. A specified mass of DMF was added to the equilibrium cell; then the equilibrium cell was evacuated again; and at last the desired amount of refrigerant was then charged into the cell. The amount of charge was such that 80 % to 90 % of the cell's volume was filled with liquid. The composition charged into the cell was therefore the composition of the liquid. The entire assembly was positioned on top of a stir plate and submerged in a thermostatted bath. The system was stirred continuously and allowed to equilibrate for 2 h before taking measurements. At low temperatures and high concentrations of DMF, they required a longer time for equilibrium. After the equilibrium, the data (temperature, pressure, and mass fraction of HFC-134a in the liquid phase) were recorded.

RESULTS AND DISCUSSION

To test the stability of the experimental system, VLE data of the binary system (HCFC-22 + DMF) were measured in the temperature range of (283.15 to 343.15) K. HCFC-22 was supplied by Honeywell Inc. (USA) with a mass purity of > 99.99 %. The data were compared with those from the literature,¹⁶ and the results were shown in Table 2 and Figure 2. From Table 2 and Figure 2, it can be seen that they kept a good agreement. In Table 2, x_1 indicates the liquid mole fraction of HCFC-22; p_{exp} is the experimental pressure; and p_{cal} is the calculated pressure.

Table 1. Critical Parameters of DMF¹⁴ and HFC-134a¹⁵

	T_c /K	P_c /MPa
DMF	650.00	5.499
HFC-134a	374.21	4.059

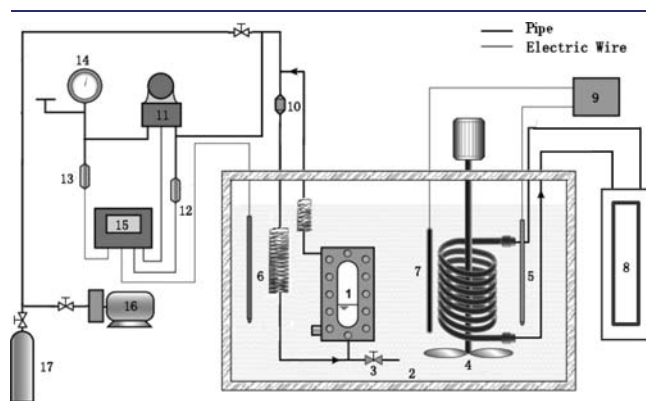


Figure 1. Schematic diagram of the experimental apparatus. 1, equilibrium cell; 2, thermostat bath; 3, valve; 4, stirrer; 5, platinum resistance thermometer; 6, calibrated platinum resistance thermometer; 7, heater; 8, refrigeration system; 9, temperature control instrument; 10, circulation pump; 11, differential-pressure sensor; 12,13, pressure sensor; 14, piston pressure gauge; 15, data collecting system; 16, vacuum pump; and 17, sample.

Table 2. Experimental Data and the Data from the Literature¹⁶ of (HCFC-22 (1) + DMF (2))

T /K	exp./kPa ($x_1 = 0.3583$)	ref./kPa ($x_1 = 0.3637$)	exp./kPa ($x_1 = 0.6596$)	ref./kPa ($x_1 = 0.6635$)
283.15	103.37	131.20	280.22	272.30
293.15	141.83	154.40	337.81	324.40
303.15	192.25	196.20	484.29	478.90
313.15	254.21	261.40	581.21	559.10
323.15	329.41	333.60	734.57	702.00
333.15	416.10	426.00	891.44	829.50
343.15	522.68	534.90	1071.93	1019.40

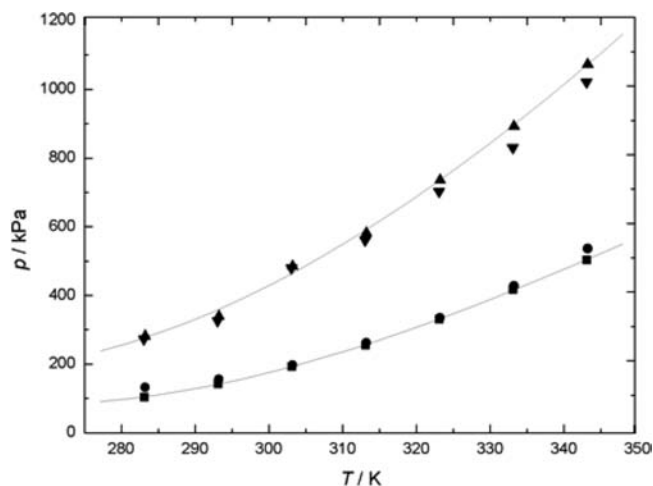


Figure 2. Solubility data of the binary system (HCFC-22 + DMF): ▼, $x = 0.6635$, literature;¹⁶ ▲, $x = 0.6596$, this work; □, $x = 0.6596$, calculated value; ■, $x = 0.3583$, this work; ●, $x = 0.3637$, literature;¹⁶ and □, $x = 0.3583$, calculated value.

In this work, the solubility data (p – T – x) were measured for the binary mixture (HFC-134a + DMF) from $T = (263.15$ to $343.15)$ K, which were shown in Table 3.

Throughout the observation of overall experiment, there was no stratification and no sediment generation, and the color of the liquid had no change in the equilibrium cell before and after the experiment. The above-mentioned content suggested that any ratio of HFC-134a and DMF could be miscible. In addition, the vapor phase of the binary mixture (HFC-134a + DMF) was analyzed using chromatography which was equipped with a Flame Ionization Detector (FID) (model: GC112A, China), where they were held at a constant temperature of 343.15 K for four days. The GC was calibrated with pure components of known purity and with mixtures of known composition that were prepared gravimetrically. The results showed that HFC-134a had no change over time, suggesting that no chemical reactions occurred. Moreover, the analysis showed there was almost no DMF in the vapor phase of the mixture.

The p – T – x data are correlated by the NRTL model¹⁷ which is expressed as follows

$$G^E = RTx_1x_2 \left[\frac{G_{21}\tau_{21}}{x_1 + G_{21}x_2} + \frac{G_{12}\tau_{12}}{x_2 + G_{12}x_1} \right] \quad (3)$$

$$\ln \gamma_1 = x_2^2 \left[\tau_{21} \left(\frac{G_{21}}{x_1 + x_2 G_{21}} \right)^2 + \frac{\tau_{12} G_{12}}{(x_2 + x_1 G_{12})^2} \right] \quad (4)$$

$$\ln \gamma_2 = x_1^2 \left[\tau_{12} \left(\frac{G_{12}}{x_2 + x_1 G_{12}} \right)^2 + \frac{\tau_{21} G_{21}}{(x_1 + x_2 G_{21})^2} \right] \quad (5)$$

where G^E is the Gibbs free energy; γ_1 and γ_2 are the activity coefficients; T is the equilibrium temperature; x_2 is the liquid mole fraction of DMF; $\tau_{12} = ((g_{12} - g_{22})/RT)$; $\tau_{21} = ((g_{21} - g_{11})/RT)$; $G_{12} = \exp(-\alpha_{12}\tau_{12})$; $G_{21} = \exp(-\alpha_{21}\tau_{21})$; and $\alpha_{12} = \alpha_{21}$.

The interactive parameters τ_{12} and τ_{21} of the NRTL model are considered as a function dependent on temperature, and

the parameter equations are as follows

$$\tau_{12} = \frac{g_{12} - g_{22}}{RT} = \frac{a_0 + a_1 \ln(T)}{RT} \quad (6)$$

$$\tau_{21} = \frac{g_{21} - g_{11}}{RT} = \frac{b_0 + b_1 \ln(T)}{RT} \quad (7)$$

where a_0 , a_1 , b_0 , and b_1 are constants.

The constants a_0 , a_1 , b_0 , and b_1 and the parameter α_{12} were obtained by minimizing the following objective function.

$$\text{OBF} = \sum_{i=1}^N \left(\frac{p_{\text{exp}} - p_{\text{cal}}}{p_{\text{exp}}} \right)_i^2 \quad (8)$$

where N is the number of experimental points; p_{exp} is the experimental pressure; and p_{cal} is the calculated pressure.

The vapor–liquid equilibria can be obtained using eq 9.

$$y_i p = \gamma_i x_i p_i^s \exp \left(\frac{V_i^L (p - p_i^s)}{RT} \right) \quad (9)$$

where p is the equilibrium pressure in MPa; p_i^s is the saturated pressure of component i in MPa; y_i is the vapor mole fraction of component i (in this paper, assumed $y_1 = 1$); x_i is the liquid mole fraction of component i ; $\exp[(V_i^L (p - p_i^s))/RT]$ is the Poynting factor; and the V_i^L value of HFC-134a is cited from REFPROP.¹⁵

In a binary solution (the case in this work), only the activity coefficient of HFC-134a in the solution (since the vapor phase is assumed to be pure refrigerant) is needed to fully describe the system. In the correlation, the saturated vapor pressure data of HFC-134a are cited from REFPROP.¹⁵ In the correlation, the least-squares algorithm is used to solve the parameters of the NRTL model.

Figures 3 to 4 and Table 2 give the correlated results and the relative pressure deviations of experimental data from the calculated values by using the NRTL model. Figure 4 gives the calculated activity coefficient of HFC-134a in DMF at different temperatures. From Figures 3 to 4 and Table 2, it can be seen that the NRTL model provides good results for the mixture (HFC-134a + DMF) with a maximum deviation of 5.2 % and an average uncertainty of 1.9 %. Meanwhile, DMF shows a high affinity with HFC-134a; for example, the molar fraction of HFC-134a in DMF at a specific temperature and pressure is higher (negative deviation) than that predicted for an ideal solution obeying Raoult's law. Still, the results from Figure 4 show that the activity coefficients are dependent on temperature. In addition, the values of the constants a_0 , a_1 , b_0 , and b_1 and the parameter α_{12} are given in Table 4. As the interactive parameters τ_{12} , τ_{21} of the NRTL model are considered as function dependent on temperature in the calculation, the correlated results showed that the NRTL model derived in the work can supply a good prediction within the wide ranges of temperatures and composition.

In addition, experimental data from Zehioua¹³ were compared with the experimental data in this work, and their ($x - \log p$) diagram for the binary system of (HFC-134a + DMF) at various compositions is shown in Figure 5. When the temperatures are (303.30, 313.18, and 323.34) K, most of the deviations are within 2.3 %; that is, they are in a good agreement with each other. However, when the temperatures are high, the deviations between them are relatively bigger, while the mole fraction of DMF is between (25 and 85) %. The biggest deviation is about 8 %.

Table 3. Vapor Pressure Data for the Mixture (HFC-134a (1) + DMF (2))

T/K	x_1	$p_{\text{exp}}/\text{kPa}$	$p_{\text{cal}}/\text{kPa}$	δp^a (%)	$\gamma_{1,\text{cal}}$
263.15	0.1496	30.10	29.17	-3.10	0.97
	0.2429	47.71	47.58	-0.27	0.98
	0.3381	67.55	66.56	-1.47	0.98
	0.4581	92.21	90.74	-1.59	0.99
	0.5673	112.73	113.00	0.24	0.99
	0.6301	123.94	125.89	1.57	1.00
	0.7377	148.10	148.06	-0.03	1.00
	0.8794	184.35	177.05	-3.96	1.00
273.15	0.1490	42.00	41.18	-1.94	0.94
	0.2422	68.24	67.33	-1.34	0.95
	0.3374	95.35	94.39	-1.00	0.96
	0.4575	128.95	129.15	0.15	0.96
	0.5671	160.60	161.55	0.59	0.97
	0.6298	181.66	180.40	-0.69	0.98
	0.7375	217.65	213.32	-1.99	0.99
	0.8793	264.69	257.12	-2.86	1.00
283.15	0.1282	47.23	48.78	3.28	0.92
	0.1919	77.14	73.27	-5.01	0.92
	0.2412	96.35	92.37	-4.14	0.92
	0.3365	130.55	129.67	-0.67	0.93
	0.4567	177.70	177.66	-0.02	0.94
	0.5667	227.35	222.78	-2.01	0.95
	0.6934	269.49	276.67	2.66	0.96
	0.7874	313.68	318.33	1.48	0.98
293.15	0.1275	63.28	65.26	3.13	0.90
	0.2359	115.98	121.36	4.64	0.90
	0.3331	169.21	172.30	1.83	0.91
	0.3842	195.78	199.40	1.85	0.91
	0.4952	255.65	259.25	1.41	0.92
	0.5273	271.00	276.87	2.17	0.92
	0.5998	309.80	317.35	2.44	0.93
	0.6932	366.72	371.35	1.26	0.94
303.15	0.7873	423.52	428.80	1.25	0.95
	0.8793	482.54	489.28	1.40	0.97
	0.9432	540.48	533.96	-1.21	0.99
	0.1267	85.15	85.39	0.29	0.88
	0.2352	155.83	159.13	2.12	0.88
	0.3324	226.83	225.86	-0.43	0.88
	0.3836	258.92	261.35	0.94	0.89
	0.4947	340.42	339.52	-0.27	0.89
313.15	0.5269	361.48	362.56	0.30	0.89
	0.5994	410.77	415.33	1.11	0.90
	0.6929	485.79	486.03	0.05	0.91
	0.7871	538.69	562.24	4.37	0.93
	0.8791	616.40	645.67	4.75	0.95
	0.9431	724.21	712.09	-1.67	0.98
	0.2343	201.58	204.52	1.46	0.86
	0.3316	296.81	290.35	-2.18	0.86
313.15	0.3828	332.16	335.85	1.11	0.87
	0.4940	442.42	435.96	-1.46	0.87
	0.5263	471.55	465.48	-1.29	0.87
	0.5989	540.62	532.92	-1.42	0.88

Table 3. Continued

T/K	x_1	$p_{\text{exp}}/\text{kPa}$	$p_{\text{cal}}/\text{kPa}$	δp^a (%)	$\gamma_{1,\text{cal}}$
323.15	0.6925	614.11	623.25	1.49	0.89
	0.7868	695.29	721.46	3.76	0.90
	0.879	801.56	832.43	3.85	0.93
	0.9424	924.69	926.11	0.15	0.97
	0.1241	135.90	137.17	0.93	0.84
	0.2316	257.57	256.38	-0.46	0.84
	0.3284	358.15	364.26	1.71	0.84
	0.3795	414.34	421.55	1.74	0.85
333.15	0.4907	561.21	547.58	-2.43	0.85
	0.523	600.62	584.67	-2.65	0.85
	0.5958	686.33	669.55	-2.45	0.85
	0.6898	793.44	783.28	-1.28	0.86
	0.7334	859.45	838.73	-2.41	0.87
	0.8778	1017.62	1050.75	3.26	0.91
	0.9418	1180.05	1179.37	-0.06	0.95
	0.1225	170.89	169.22	-0.98	0.83
343.15	0.2287	328.31	316.17	-3.70	0.83
	0.3249	470.70	449.78	-4.44	0.83
	0.3758	541.95	520.81	-3.90	0.83
	0.4869	682.27	677.21	-0.74	0.83
	0.5194	743.01	723.57	-2.62	0.83
	0.5924	845.63	829.08	-1.96	0.83
	0.6787	973.41	957.99	-1.58	0.84
	0.7214	1019.21	1024.49	0.52	0.85
353.15	0.8764	1265.18	1305.15	3.16	0.89
	0.9412	1490.86	1475.00	-1.06	0.93
	0.1201	200.13	204.41	2.14	0.81
	0.2249	404.16	383.00	-5.23	0.81
	0.3204	568.42	546.26	-3.90	0.81
	0.3711	653.26	633.29	-3.06	0.81
	0.4821	809.19	825.39	2.00	0.81
	0.5148	896.01	882.74	-1.48	0.81
363.15	0.5881	1005.62	1012.74	0.71	0.82
	0.6748	1221.11	1171.64	-4.05	0.82
	0.7173	1305.10	1252.62	-4.02	0.83
	0.8746	1590.13	1599.67	0.60	0.87
	0.9405	1858.13	1816.72	-2.23	0.91
	0.1165	235.11	241.22	2.60	0.79
	0.2125	425.66	440.33	3.45	0.79
	0.3139	651.57	651.50	-0.01	0.79
363.15	0.3643	768.09	756.98	-1.45	0.79
	0.4752	958.99	990.88	3.33	0.80
	0.5082	1016.92	1061.24	4.36	0.80
	0.5818	1195.43	1220.31	2.08	0.80
	0.6693	1430.14	1415.02	-1.06	0.81
	0.7121	1520.30	1513.68	-0.44	0.81
	0.8721	1955.90	1938.36	-0.90	0.85
	0.9393	2286.35	2208.00	-3.43	0.89
363.15	0.1111	280.11	276.79	-1.19	0.78
	0.2018	503.14	503.67	0.11	0.78
	0.3048	752.25	762.76	1.40	0.78
	0.3550	891.72	889.85	-0.21	0.78
	0.4659	1149.12	1172.99	2.08	0.78
	0.4992	1227.36	1258.93	2.57	0.78

Table 3. Continued

T/K	x_1	$p_{\text{exp}}/\text{kPa}$	$p_{\text{cal}}/\text{kPa}$	δp^a (%)	$\gamma_{1,\text{cal}}$
	0.5734	1415.89	1452.74	2.60	0.79
	0.6619	1631.87	1689.92	3.56	0.79
	0.7041	1738.41	1806.75	3.93	0.80
	0.8686	2315.66	2325.86	0.44	0.83
	0.9375	2715.84	2654.10	-2.27	0.87

$$^a \delta p = ((p_{\text{exp}} - p_{\text{cal}})/p_{\text{exp}}) \times 100.$$

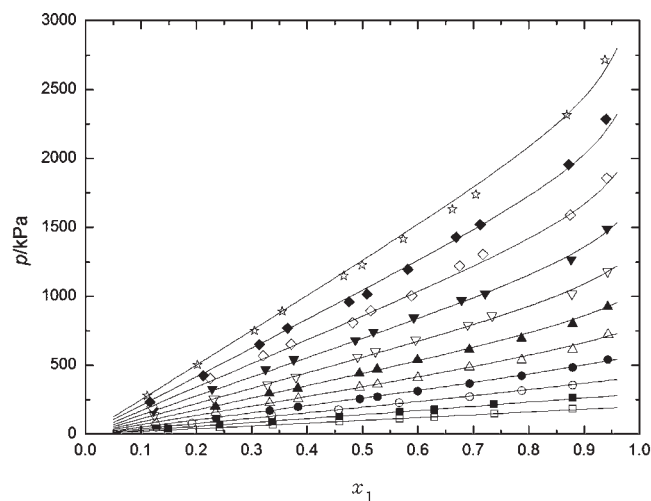


Figure 3. Solubility of HFC-134a in DMF as a function of temperature: □, 263.15 K; ■, 273.15 K; ○, 283.15 K; ●, 293.15 K; △, 303.15 K; ▲, 313.15 K; ▽, 323.15 K; ▼, 333.15 K; ◇, 343.15 K; ◆, 353.15 K; and ☆, 363.15 K; solid line, calculated results using the NRTL model.

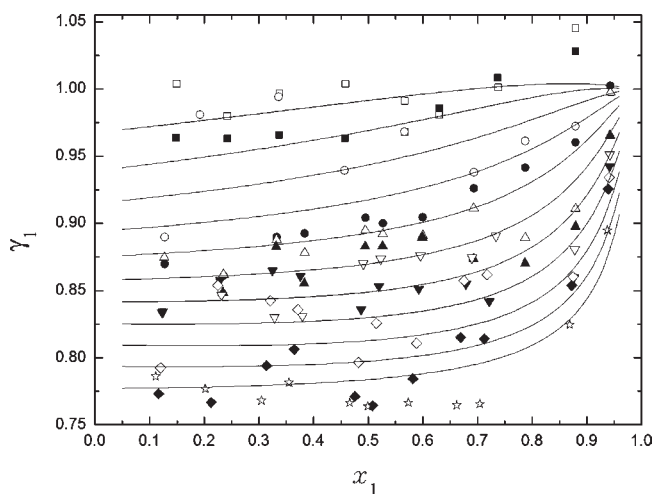


Figure 4. Activity coefficient of HFC-134a in DMF as a function of mole fraction and temperature at different temperatures using the NRTL model: □, 263.15 K; ■, 273.15 K; ○, 283.15 K; ●, 293.15 K; △, 303.15 K; ▲, 313.15 K; ▽, 323.15 K; ▼, 333.15 K; ◇, 343.15 K; ◆, 353.15 K; and ☆, 363.15 K; solid line, calculated activity coefficient of HFC-134a.

Meanwhile, by analyzing the data, it can be seen that the experimental data from Zehioua suggest that the mixture of (HFC-134a + DMF) is close to the ideal solution, while the experimental data from this paper suggest that DMF shows

Table 4. Constant Values Derived by Fitting the Experimental Data and Experimental Data Range

model	constant values					experimental data range	
	a_0	a_1	b_0	b_1	α_{12}	temp./K	mole fraction
NRTL	8073	-1367	11638	-2106	14	263.15 to 363.15	0.1 to 0.95

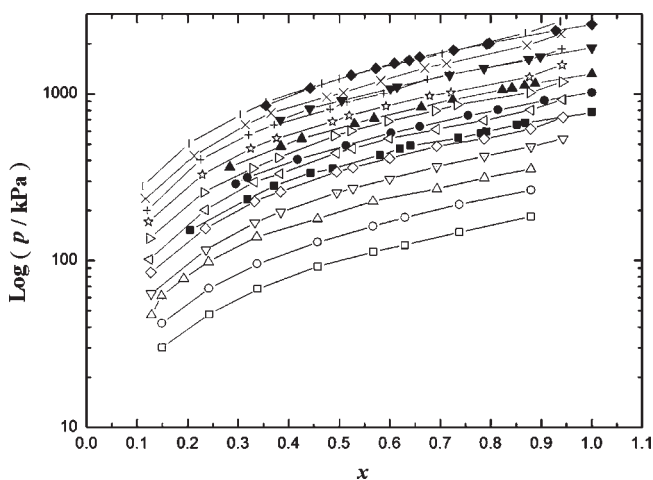


Figure 5. $(x - \log p)$ diagram for the mixture (HFC-134a + DMF). In the literature: ■, 303.30 K; ●, 313.18 K; ▲, 323.34 K; ▼, 338.26 K; ◆, 353.24 K. In this work: □, 263.15 K; ○, 273.15 K; △, 283.15 K; ▽, 293.15 K; ◇, 303.15 K; open triangle pointing left, 313.15 K; open triangle pointing right, 323.15 K; ☆, 333.15 K; +, 343.15 K; ×, 353.15 K; |, 363.15 K.

very high affinity with HFC-134a because the mole fraction of HFC-134a in DMF at a specific temperature and pressure is higher (negative deviation) than that predicted for an ideal solution obeying Raoult's law.

CONCLUSIONS

In this paper, the vapor–liquid equilibrium data of the different mass fractions of the mixture (HFC-134a + DMF) in the temperature range of (263.15 to 363.15) K were measured. In the experiment, there was no stratification and no sediment generation in the liquid phase of the mixture, and the color of the liquid phase of the mixture had no change in the equilibrium cell before and after the experiment. Moreover, using the NRTL model, the experimental data were correlated, and the results showed that the overall average relative deviation of the pressure by NRTL is 1.9 % and that its maximum relative deviation of the pressure is 5.2 %. The predicted results show a good agreement with the experimental data. It is shown that HFC-134a indicates a very good solubility characteristic with DMF as the solvent, and the mixture has a negative deviation from Raoult's law. This work will be a good extension and play an important role in the refrigerant system for a wide temperature and composition range.

AUTHOR INFORMATION

Corresponding Author

*Tel.: +86 571 8795 1680. Fax: +86 571 8795 2464. E-mail: gmchen@zju.edu.cn.

Funding Sources

This work is financially supported by National Basic Research Program of China under award No. 2010CB227304. The support of the Excellent Young Teachers Program of Zhejiang University (Zijin program) is gratefully acknowledged.

REFERENCES

- (1) Eiseman, B. J. Why R22 should be favored for absorption refrigeration. *ASHRAE J.* **1959**, *12*, 45–50.
- (2) Bhaduri, S. C.; Varma, H. K. P–T–X behavior of refrigerant-absorbent pairs. *Int. J. Refrig.* **1985**, *8*, 172–175.
- (3) Agarwal, R. S.; Bapat, S. L. Solubility characteristics of R22–DMF refrigerant-absorption combination. *Int. J. Refrig.* **1985**, *8*, 70–74.
- (4) Bhaduri, S. C.; Verma, H. K. P–T–X behavior of R22 with five different absorptions. *Int. J. Refrig.* **1986**, *9*, 362–366.
- (5) Jelinek, M.; Borde, I.; Yaron, I. Enthalpy-concentration diagram of the system R22–DIMETHYL FORMAMIDE and performance characteristics of refrigeration cycle operating with this system. *ASHRAE Trans.* **1978**, *84*, 60–67.
- (6) Bhaduri, S. C.; Verma, H. K. Heat of mixing of R22-absorbent mixture. *Int. J. Refrig.* **1988**, *11*, 181–185.
- (7) Fatuh, M.; Murthy, S. S. Comparison of R22-absorbent pairs for vapor absorption heat transformers based on P–T–X data. *Heat Recovery Syst. CHP* **1993**, *13*, 33–48.
- (8) Mark, O. M.; Eric, W. L.; Richard, T. J. Thermodynamic properties for the alternative refrigerants. *Int. J. Refrig.* **1998**, *21*, 322–338.
- (9) Borde, I.; Jelinek, M.; Daltrophe, N. C. Absorption system based on the refrigerant R134a. *Int. J. Refrig.* **1995**, *18*, 387–394.
- (10) Domanski, P. A. Refrigerants for the 21st Century/ASHRAE/NIST Refrigerants Conference. *J. Res. Natl. Inst. Stand. Technol.* **1998**, *103*, 529–533.
- (11) Tillner, R.; Li, J.; Yokozeki, A.; Sato, H.; Watanabe, K. *Thermodynamic properties of pure and blended hydrofluorocarbon (HFC) refrigerants*; Japan society of refrigerating and air conditioning engineers: Tokyo, 1998.
- (12) Peng, D. Y.; Robinson, D. B. A new two-constant equation of state. *Ind. Eng. Chem. Fundam.* **1976**, *15*, 59–64.
- (13) Zehioua, R.; Coquelet, C.; Meniai, A.-H.; Richon, D. Isothermal Vapor-Liquid Equilibrium Data of 1,1,1,2-Tetrafluoroethane (R134a) + Dimethyl- formamide (DMF) Working Fluids for an Absorption Heat Transformer. *J. Chem. Eng. Data* **2010**, *55*, 985–988.
- (14) *Dortmund Data Bank (DDB)*, version 97; DDBST Software and Separation Technology GmbH: Oldenburg, Germany, 1997.
- (15) Lemmon, E. W.; Huber, M. L.; McLinder, M. O. *NIST Reference Fluid Thermodynamic and Transport Properties Database - REFPROP*, version 7.0; National Institute of Standards and Technology: Maryland, USA, 2002.
- (16) Agarwal, R. S.; Bapat, S. L. Solubility characteristics of R22-DMF refrigerant-absorption combination. *Int. J. Refrig.* **1985**, *8*, 70–74.
- (17) Renon, H.; Prausnitz, J. M. Local compositions in thermodynamic excess functions for liquid mixtures. *AIChE J.* **1968**, *14*, 135–144.